Available online at www.sciencedirect.com
ScienceDirect
Trans. Nonferrous Met. Soc. China 25(2015) 2214−2220
Transactions of Nonferrous Metals Society of China
www.tnmsc.cn

Effect of Nb addition on microstructure, mechanical properties and castability of β-type Ti−Mo alloys

Ling-bo ZHANG[1], Ke-zheng WANG[2], Li-juan XU[3], Shu-long XIAO[3], Yu-yong CHEN[3]

1. Stomatology Department, 2nd Affiliated Hospital, Harbin Medical University, Harbin 150086, China;
2. Department of Radiology, 4th Affiliated Hospital, Harbin Medical University, Harbin 150001, China;
3. School of Materials Science and Engineering, Harbin Institute of Technology, Harbin 150001, China

Received 10 June 2014; accepted 10 April 2015

Abstract: To develop novel β-type biomedical titanium alloys, a series of Ti−15Mo−xNb alloys(x=0, 5, 10 and 15, mass fraction in %) were designed and prepared by using vacuum arc melting method. The present study focused on the effect of Nb addition on the microstructure, mechanical properties and castability of Ti−15Mo alloy. Phase analysis and microstructure observation show that all the alloys consist of single β phase and the equiaxed β grain is refined with increasing Nb content. These β-type Ti−15Mo−xNb alloys exhibit good plasticity and rather low compression elastic modulus (in the range of 18.388−19.365 GPa). After Nb addition, the compression yield strength of the alloys increases. With increasing Nb content, the micro-hardness of the alloys decreases. The alloys exhibit obvious fibrous strip microstructure after cold compression deformation. The castability test shows that the castability of the alloys after Nb addition decreases and that of the Ti−15Mo alloy is the highest (92.01%).
Key words: β-titanium alloys; Ti−Mo−Nb; Nb; castability; microstructure; mechanical properties

1 Introduction

Ti and Ti alloys are extensively used in a variety of application fields like aerospace, chemical industries and many medical applications because of their good biocompatibility, excellent mechanical properties and corrosion resistance [1,2]. CP-Ti is used extensively in dental applications but is found not to be suitable for load bearing applications owing to its poor mechanical properties such as low shear strength [2]. Ti−6Al−4V alloy is the most widely used titanium alloy in the orthopedic applications, but the release of Al and V ions from the alloy in the human body might cause cytotoxic effects [2−4], and also increases the potential for the development of Alzheimer's disease especially during long-term implantation[2]. The most promising materials for biomedical applications are the multifunctional β-Ti alloys [2]. More recently, a great deal of studies have focused on the development of β and near-β phase titanium alloys with non-toxic elements such as Mo, Nb, Zr, Sn and Ta. Some new near β-type Ti alloys containing β-stabilizers such as Mo, Nb and Zr have attracted much advantages for orthopedic implant applications including better mechanical properties, low elastic modulus, superior biocorrosion resistance and excellent biocompatibility[2,4−7].

Molybdenum (Mo) shows β stabilizing properties in Ti alloys, and thus it is an effective β stabilizer for designing β-type alloys [8]. Nb is non-toxic and non-allergic and also can stabilize β phase showing low elasticity modulus and great strength [3]. Moreover, it is well known that β-stabilizer Mo and Nb elements can form homogenous solid solution with Ti in all kinds of Ti alloys when they are alloyed within certain concentration [2]. In recent years, Ti−Mo [9], Ti−Mo−Nb [10] and Ti−Mo−Ta [7] alloys have been researched with emphasis on their microstructure, mechanical properties and corrosion resistance for medical applications. Many studies have shown excellent mechanical compatibility of Ti alloys containing Mo [9−13], such as Ti−15Mo [11], Ti−10Mo−10Nb [10] and Ti−12Mo−5Ta [7]. The metastable β phase Ti−15Mo alloy showed low modulus and extremely high corrosion

Foundation item: Project (QN2010-04) supported by the Youth Startup Fund of the Second Affiliated Hospital of Harbin Medical University, China; Project (2010-156) supported by the Medical Scientific Research Foundation of Heilongjiang Province Health Department, China; Project (HIT.NSRIF.2012002) supported by the Fundamental Research Funds for the Central Universities, China
Corresponding author: Li-juan XU; Tel/Fax: +86-451-86418802; E-mail: xljuan@hit.edu.cn
DOI: 10.1016/S1003-6326(15)63834-1

resistance [9]. In this regard, the addition of Mo and Nb is preferable to developing absolutely safe Ti-based alloys for biomedical applications depending upon its ability to achieve biological passivity and capacity of reducing the elastic modulus [2].

In terms of applications of biomaterials, the mechanical properties and castability of the alloys most need to study. The purpose of this study is to investigate the effect of Nb addition on the microstructure, mechanical properties and castability of β-type Ti−15Mo alloy as biomedical materials.

2 Experimental

The designed alloys, namely Ti−15Mo−xNb (x=0, 5, 10 and 15, mass fraction in %), were prepared by mixing an appropriate amount of high-purity sponge Ti (99.8%), Mo piece (99.9%) and Nb piece (99.9%). The mixtures were melted under a high-purity argon atmosphere in a vacuum non-consumable arc melting furnace. The ingots were inverted and remelted at least four times to maintain homogenized. After vacuum arc melting, the alloy ingots were centrifugally cast into a graphite mold by using a centrifugal titanium casting machine.

The alloy ingots were sectioned by using electrospark-erosion. The phase identification was carried out by X-ray diffraction (XRD) using Cu K_α radiation at an accelerating voltage of 40 kV and a current of 250 mA. Micro-hardness was measured using a hardness tester (CLEMEX, MMT-X78) with a load of 0.98 N and a dwell time of 15 s. Compression tests were determined on INSTRON 5500 compression instrument at a rate of 0.5 mm/min and room temperature. The dimensions of compression specimens were d4 mm × 6 mm. All the samples were cold deformed to 50% engineering strain during compression tests. The optical microstructure after compression deformation was carried out on the plane taken from the mid-section of the deformed samples. The specimens for observing microstructure were mechanically polished using SiC waterproof papers (grade from 240 to 2000), finished by polishing with electrolytic etching and eroded with 8% HF + 15% HNO_3 + 77% H_2O. Microstructure of the etched specimens was examined using an optical microscope (OM, OLYMPUS BH2-UMA) and a scanning electron microscope (SEM, FEI Quanta 200F).

The castability of Ti−15Mo−xNb alloys was investigated by modified Whitlock's method [14]. The schematic view of mesh-pattern wax mold is shown in Fig. 1(a). Wax patterns used in this study were produced by injecting wax into an aluminum metal mold on a wax injection machine, as shown in Fig. 1(b). In this study, the wax mesh with 169 square shaped spaces of 2 mm × 2 mm was selected. The bilateral wax runner bars with 3 mm in diameter were attached to both edges of the wax mesh. The dominate wax runner bar with 5 mm in diameter and 5 mm in length was attached to the corner of wax mesh. After the mesh-pattern wax mold was obtained, the ceramic mold was fabricated according to the traditional investment casting process. CaO-stabilized ZrO_2 powders mixed with zirconia sol binder were prepared for the primary coating slurry. Mullite refractory and colloidal silica binders were prepared for the back-up layers. A centrifugal titanium casting machine (LZ5, made by Luoyang Ming Tao Science and Technology Co. Ltd., China) was used to cast the series of materials, with about 30 g alloy and 30 s melting time for each casting. All casting experiments were carried out under the same conditions.

The castability was calculated by Whitlock's formula [4]. It can be illustrated in Fig. 1 that the wax mesh provides a grid with 169 open squares and 338 segments. After casting, the number of complete cast segments (n) was counted, divided by 338, and multiplied by 100% to obtain a percentage designated as castability value (C), as shown in Eq. (1). The segment was deemed to be complete or incomplete according to the previous work [14].

$$C=\frac{n}{338}\times 100\% \quad (1)$$

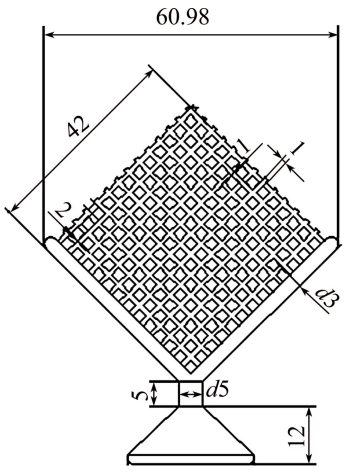

Fig. 1 Schematic view of mesh-pattern wax mold (unit: mm)

3 Results and discussion

3.1 Microstructure and mechanical properties of Ti−15Mo−xNb alloys

Figure 2 shows the XRD patterns of the Ti−15Mo−xNb alloys. There is no indication that α phase peaks or any intermediate phase peaks are included in any of the present XRD patterns. Only peaks corresponding to the body-centered-cubic (BCC) single β phase are detected and the corresponding diffraction

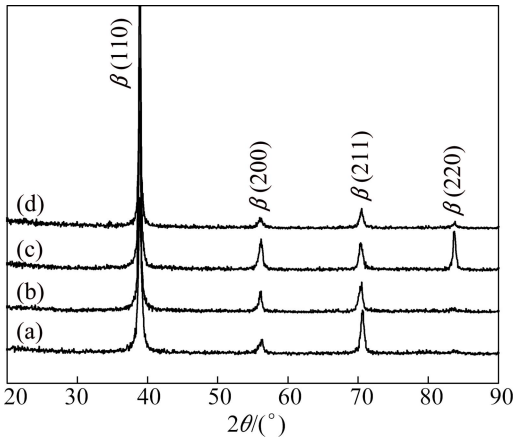

Fig. 2 XRD patterns of Ti−15Mo−*x*Nb alloys: (a) *x*=0; (b) *x*=5; (c) *x*=10; (d) *x*=15

planes, such as (110), (200), (211) and (220) can be well identified in each alloy specimen. As Ti, Mo and Nb have the same structure-type, space group and similar crystal lattice, they may completely dissolve with each other and form the metastable *β* phase at high temperatures [15]. Moreover, Mo and Nb are *β* stabilizing elements which can stabilize *β* phase. The value of *β*-stabilizer equivalence of Ti−15Mo−*x*Nb alloys is higher than 10.0%, which classifies the alloy in the *β*-metastable category [4].

Optical micrographs of the Ti−15Mo−*x*Nb alloys are shown in Fig. 3. All four alloys are composed of the single *β* phase with equiaxed grain size of 50−100 μm. The equiaxed grain boundary is very clear. These observations agree well with the results obtained from Fig. 2. SEM micrographs in BSE mode of four experimental alloys are shown in Fig. 4. Increasing Nb content resulted in the refinement of *β* grain. It has been reported that Nb additions decrease the grain size in Ti−*x*Nb−3Zr−2Ta alloys [16]. The etched granular structure is obviously observed in Ti−15Mo−10Nb and Ti−15Mo−15Nb alloys with high Nb content. The *β* phase grain size decreases with increasing Nb content, possibly due to Nb-grain boundary interaction that slows down the growth of the grain boundaries. The difference of etched granular structure of high Nb alloys is a direct result of chemical microsegregation that occurred during the formation of dendrites [1].

Typical room-temperature compression stress−strain curves of Ti−15Mo−*x*Nb alloys are shown in Fig. 5. All the alloys present a very high ductility in compression and they could be compressed to around 50% without any crack appearance. Table 1 shows the main performances of Ti−15Mo−*x*Nb alloys. After element Nb addition, the micro-hardness decreases with increasing Nb content. Ti−15Mo alloy has the highest micro-hardness (HV 334) and that of Ti−15Mo−15Nb alloy is the lowest (HV 262). In the series of alloys, the lowest compression elastic modulus is found in the Ti−15Mo alloy (18.388 GPa). The values of compression elastic modulus of Ti−15Mo−10Nb and Ti−15Mo−15Nb

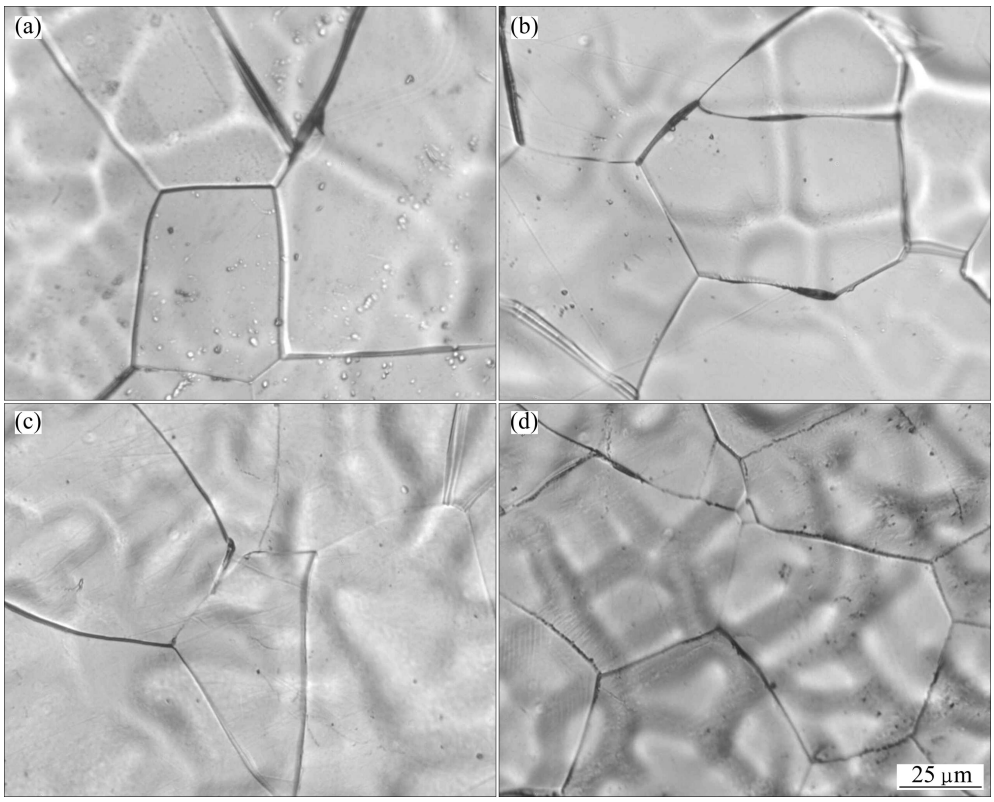

Fig. 3 Optical micrographs of Ti−15Mo−*x*Nb alloys: (a) *x*=0; (b) *x*=5; (c) *x*=10; (d) *x*=15

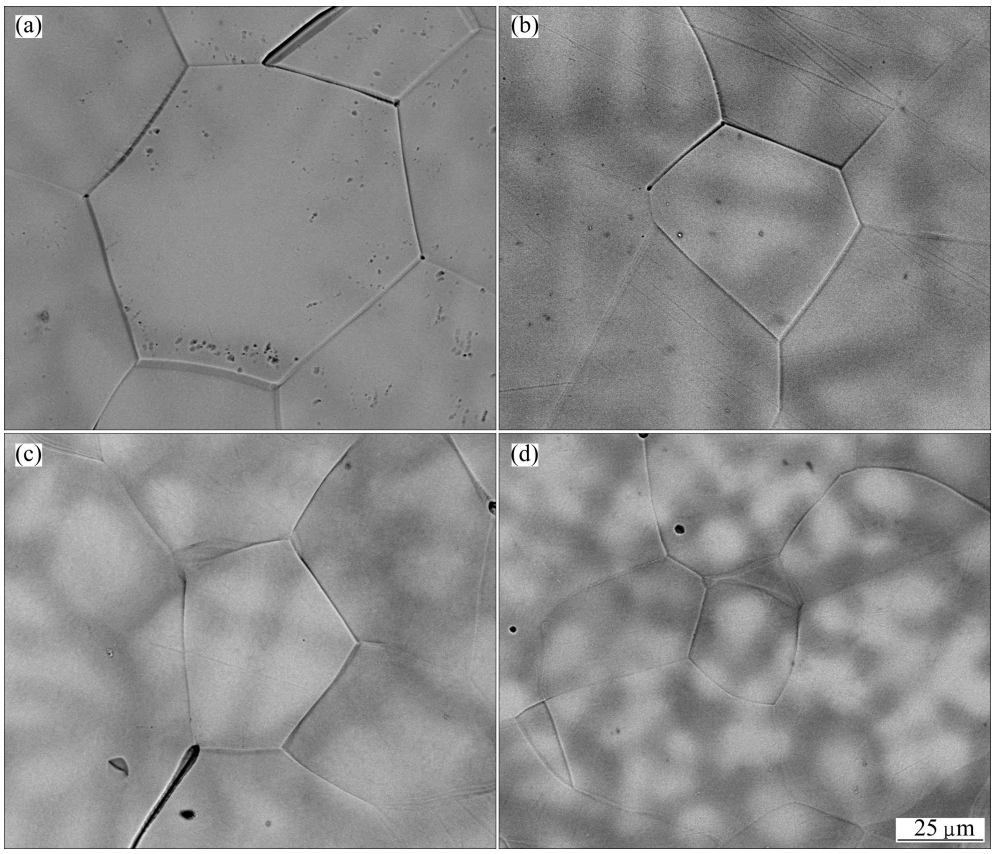

Fig. 4 SEM micrographs in BSE mode of Ti−15Mo−*x*Nb alloys: (a) *x*=0; (b) *x*=5; (c) *x*=10; (d) *x*=15

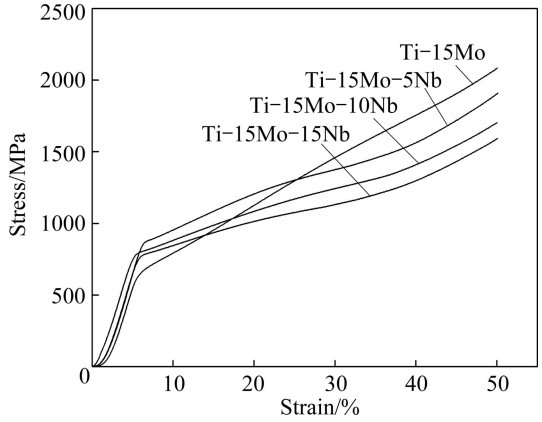

Fig. 5 Room-temperature compression stress−strain curves of Ti−15Mo−*x*Nb alloys

alloys are very similar with that of Ti−15Mo alloy, and the Ti−15Mo−5Nb alloy has the highest compression elastic modulus (19.365 GPa). Because the ductility of the series of alloys samples is very high, the rupture did not happen in all alloy samples during the compression tests with cold deformation to 50% engineering strain. After 50% cold deformation, Ti−15Mo alloy has the lowest compression yield strength (617.89 MPa) and the highest compression strength (2084.57 MPa). While with the addition of Nb, the compression yield strength increases. Ti−15Mo−5Nb alloy has the highest compression yield strength (860.32 MPa). The compression yield strength of Ti−15Mo−15Nb only is 708.47 MPa, but the value is still 14.66% higher than that of Ti−15Mo alloy. Moreover, the compression strength decreases with increasing Nb content, and the values of the series alloys are 1908.02, 1703.25 and 1592.46 MPa, respectively. The compression strength is not the strength of alloy samples ruptured, which only exhibits that the alloys have a very high ductility in compression and without any cracking after being compressed to 50%. Therefore, the compression yield strength and compression strength are different. XU et al [10] indicated that the Vickers hardness presents the reduced tendency with increasing Nb content. The compressive strength, yield strength and elastic modulus of Ti−Mo−Nb alloys reduce with increasing Nb content. The isomorphous stabilizers of Mo and Nb can improve the strength and reduce the elastic modulus.

Figure 6 exhibits the optical microstructures of the Ti−15Mo−*x*Nb alloys after compression deformation. After 50% cold compression deformation, the grains of the alloys are elongated and exhibit microstructure with obvious fibrous strip due to the large deformation. Generally speaking, the samples present deformation heterogeneities, such as shear bands, which occurred in

more strongly deformed samples. These bands are important deformation heterogeneities which act as preferential nucleation sites for recrystallization when the previously deformed material is subjected to high temperatures [17]. Moreover, it is reported that cold deformation can enhance the strength and reduce the elastic moduli of β-type titanium alloys at the same time. When the titanium alloy deforms to a certain extent, the twin and subgrain generate and refine continuously, and change to the large angle grain boundary ultimately, resulting in the formation of fibrous microstructures and grain refinement [18].

3.2 Castability of Ti−15Mo−*x*Nb alloys

Figure 7 shows the images of mesh-pattern castings of experimental Ti−15Mo−*x*Nb alloys. It is obvious that the Ti−15Mo alloy has more complete casting segments than others. Figure 8 exhibits the castability values of as-cast Ti−15Mo, Ti−15Mo−5Nb, Ti−15Mo−10Nb and Ti−15Mo−15Nb alloys, which are 92.01%, 79.88%, 66.27%, and 47.63%, respectively. It can be seen that Ti−15Mo alloy displays the highest castability value. The castability value of Ti−15Mo−5Nb alloy is little lower than that of Ti−15Mo alloy. However, with further increasing the Nb content, the castability values of Ti−15Mo−10Nb and Ti−15Mo−15Nb alloys reduce obviously.

The castability of an alloy is often associated with its ability to fill the mold. The numerous factors, such as mold design, mold temperature, cooling rate, molten metal temperature, mold reaction, type of machine, applied pressure, surface tension (surface free energy) and oxide film of alloy affect the mold filling [19]. In this study, in order to compare the castability of Ti−15Mo−*x*Nb alloys, the casting process parameters were fixed. Mold reaction, surface tension, oxide film of alloy and the Nb addition are the most likely affecting factors of castability. The alloy with slighter mold

Table 1 Performance of Ti−15Mo−*x*Nb alloys

Alloy	Micro-hardness (HV)	Compression elastic modulus/GPa	Compression yield strength/ MPa	Compression strength/MPa
Ti−15Mo	334	18.388	617.89	2084.57
Ti−15Mo−5Nb	323	19.365	860.32	1980.02
Ti−15Mo−10Nb	272	18.396	762.88	1703.25
Ti−15Mo−15Nb	262	18.651	708.47	1592.46

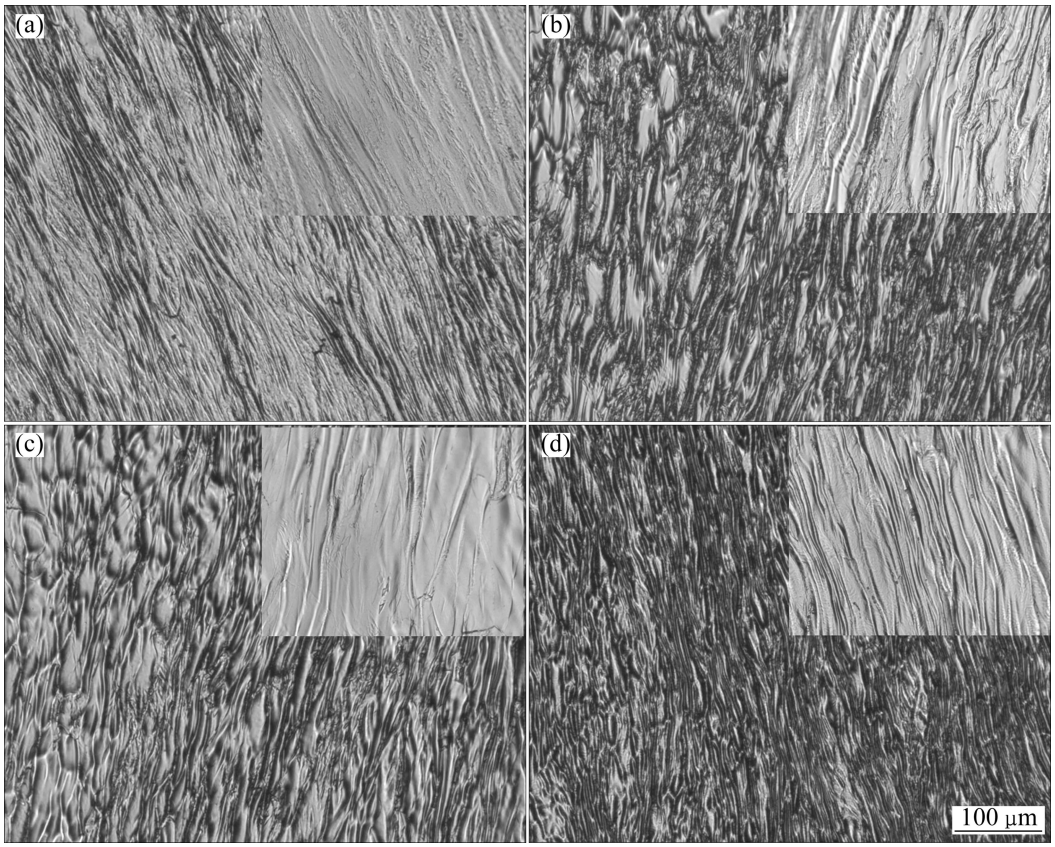

Fig. 6 Optical compression deformation microstructures of Ti−15Mo−*x*Nb alloys: (a) *x*=0; (b) *x*=5; (c) *x*=10; (d) *x*=15

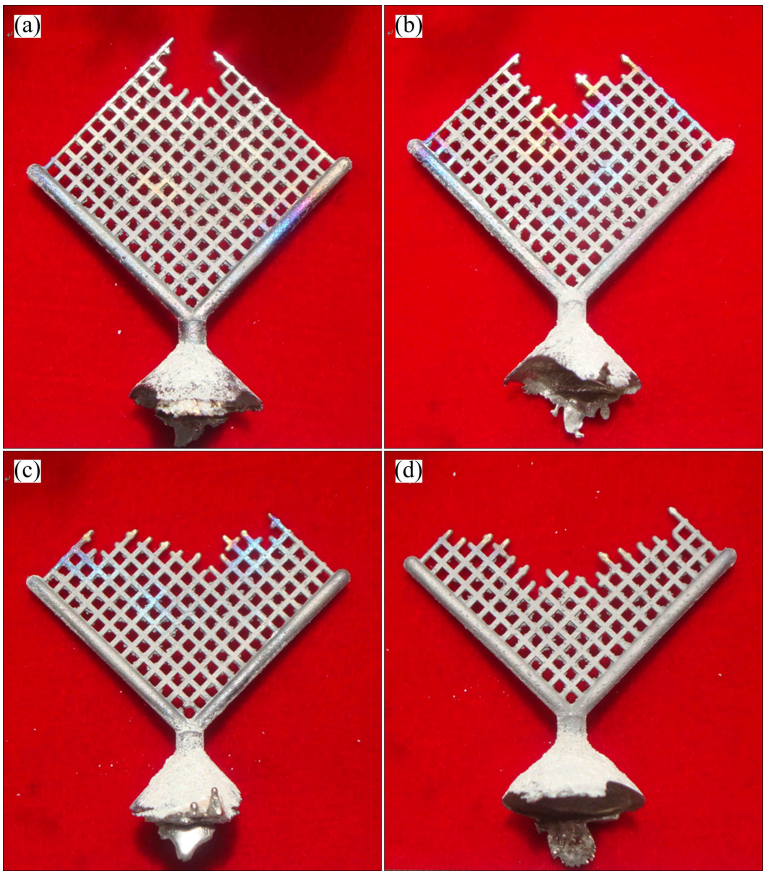

Fig. 7 Images of mesh-pattern castings of Ti−15Mo−*x*Nb alloys: (a) *x*=0; (b) *x*=5; (c) *x*=10; (d) *x*=15

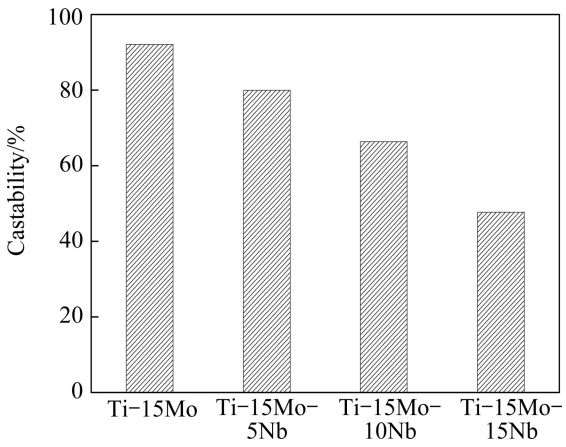

Fig. 8 Castability of as-cast Ti−15Mo−*x*Nb alloys

reaction, lower surface energy and more complete oxide film has better castability. Moreover, according to the casting theory, the Nb element addition increases the crystallization temperature of alloy. At the same degree of superheat, the liquidity of the alloy will be reduced by adding alloying elements, that is to say, the castability is also reduced. This is due to the fact that the solidification no longer occurs at the solidification interface and the generation of the dendritic structure in the preliminary stage of the solidification process will make the molten metal flow more difficult. Another possible factor is that adding alloying element Nb changes the surface oxidation film characteristics of the alloy, and further affects its castability [20]. These factors can explain why the castability decreases in the studied Ti−15Mo−*x*Nb alloys with increasing Nb content.

4 Conclusions

1) The Ti−15Mo−*x*Nb alloys consist of the single β phase and exhibit equiaxed β phase structure. The grain size decreases with increasing Nb content.

2) All the alloys have good plasticity, high yield strength and low compression elastic modulus. Ti−15Mo alloy has the lowest compression yield strength and Ti−15Mo−5Nb alloy has the highest compression yield strength. These β-type Ti−15Mo−*x*Nb alloys have low compression elastic modulus in the range of 18.388−19.365 GPa. The micro-hardness decreases with increasing Nb content. Ti−15Mo alloy has the highest micro-hardness and that of Ti−15Mo−15Nb alloy is the lowest (HV 262). After 50% cold compression deformation, all the alloys exhibit microstructure with obvious fibrous strip due to the large deformation.

3) After Nb addition, the castability of the Ti−15Mo−*x*Nb alloys decreases. Ti−15Mo alloy exhibits the highest castability (92.01%). With increasing Nb

content, the castability of the Ti−15Mo−*x*Nb alloys obviously reduces and that of Ti−15Mo−15Nb is 47.63%.

References

[1] LIN D J, CHERN LIN J H, JU C P. Structure and properties of Ti−7.5Mo−*x*Fe alloys [J]. Biomaterials, 2002, 23(8): 1723−1730.

[2] MOHAMMED M T, KHAN Z A, GEETHA M. Effect of thermo-mechanical processing on microstructure and electrochemical behavior of Ti−Nb−Zr−V new metastable *β* titanium biomedical alloy [J]. Transactions of Nonferrous Metals Society of China, 2015, 25(3): 759−769.

[3] ZHAO Chang-li, ZHANG Xiao-nong, CAO Peng. Mechanical and electrochemical characterization of Ti−12Mo−5Zr alloy for biomedical application [J]. Journal of Alloys and Compounds, 2011, 509(32): 8235−8238.

[4] GABRIEL S B, PANAINO J V P, SANTOS I D, ARAUJO L S, MEI P R, de ALMEIDA L H, NUNES C A. Characterization of a new beta titanium alloy, Ti−12Mo−3Nb, for biomedical applications [J]. Journal of Alloys and Compounds, 2011, 536(S1): s208−s210.

[5] ZHOU Y L, NIINOMI M, AKAHORI T, FUKUI H, TODA H. Corrosion resistance and biocompatibility of Ti−Ta alloys for biomedical applications [J]. Materials Science and Engineering A, 2005, 398(1−2): 28−36.

[6] AFONSO C R M, ALEIXO G T, RAMIREZ A J, CARAM R. Influence of cooling rate on microstructure of Ti−Nb alloy for orthopedic implants [J]. Materials Science and Engineering C, 2007, 27(4): 908−913.

[7] MARECI D, CHELARIU R, CAILEAN A, BRINZA F, BOLAT G, GORDIN D M. Electrochemical characterization of Ti12Mo5Ta alloys in contact with saline medium[J]. Transactions of Nonferrous Metals Society of China, 2015, 25(1): 345−352.

[8] ZHAO X F, NIINOMI M, NAKAI M, HIEDA J. Beta type Ti−Mo alloys with changeable Young's modulus for spinal fixation applications [J]. Acta Biomaterialia, 2012, 8(5): 1990−1997.

[9] OLIVEIRA N T C, GUASTALDI A C. Electrochemical stability and corrosion resistance of Ti−Mo alloys for biomedical applications [J]. Acta Biomaterialia, 2009, 5(1): 399−405.

[10] XU L J, CHEN Y Y, LIU Z G, KONG F T. The microstructure and properties of Ti−Mo−Nb alloys for biomedical application [J]. Journal of Alloys and Compounds, 2008, 453(1−2): 320−324.

[11] HO W F, JU C P, CHERN LIN J H. Structure and properties of cast binary Ti−Mo alloys [J]. Biomaterials, 1999, 20(22): 2115−2122.

[12] LIN D J, CHUANG C C, CHERN LIN J H, LEE J W, JU C P, YIN H S. Bone formation at the surface of low modulus Ti−7.5Mo implants in rabbit femur [J]. Biomaterials, 2007, 28(16): 2582−2589.

[13] GORDIN D M, GLORIANT T, TEXIER G, THIBON I, ANSEL D, DUVAL J L, NAGEL M D. Development of a *β*-type Ti−12Mo−5Ta alloy for biomedical applications: Cytocompatibility and metallurgical aspects [J]. Journal of Materials Science: Materials in Medicine, 2004, 15(8): 885−891.

[14] HINMAN R W, TESK J A, WHITLOCK R P, PARRY E E, DURKOWSKI J S. A technique for characterizing casting behavior of dental alloys [J]. Journal of Dental Research, 1985, 64(2): 134−138.

[15] LI Chun-liu, ZHAN Yong-zhong, JIANG Wen-ping. *β*-type Ti−Mo−Si ternary alloys designed for biomedical applications [J]. Materials and Design, 2012, 34(2): 479−482.

[16] ZHU Y F, WANG L Q, WANG M M, LIU Z T, QIN J N, ZHAND D, LV W J. Superelastic and shape memory properties of Ti*x*Nb3Zr2Ta alloys [J]. Journal of the Mechanical Behavior of Biomedical Materials, 2012, 12: 151−159.

[17] HAYAMA A O F, LOPES J F S C, GOMES DA SILVA M J, ABREU H F G, GARAM R. Crystallographic texture evolution in Ti−35Nb alloy deformed by cold rolling [J]. Materials and Design, 2014, 60: 653−660.

[18] ZHEREBTSOV S V, DYAKONOV G S, SALEM A A, MALYSHEVA S P, SALISHCHEV G A, SEMIATIN S L. Evolution of grain and subgrain structure during cold rolling of commercial-purity titanium [J]. Materials Science and Engineering A, 2011, 528(9): 3474−3479.

[19] OLIVEIRA P C G, ADABO G L, RIBEIRO R F, ROCHA S S. The effect of mold temperature on castability of CP Ti and Ti−6Al−4V castings into phosphate bonded investment materials [J]. Dental Materials, 2006, 22(12): 1098−1102.

[20] CHENG W W, CHERN LIN J H, JU C P. Bismuth effect on castability and mechanical properties of Ti−6Al−4V alloy cast in copper mold [J]. Materials Letters, 2003, 57(16−17): 2591−2596.

Nb 元素对 *β* 型 Ti−Mo 基合金显微组织、力学性能和铸造性能的影响

张令波[1]，王可铮[2]，徐丽娟[3]，肖树龙[3]，陈玉勇[3]

1. 哈尔滨医科大学 附属第二医院 口腔科，哈尔滨 150086；
2. 哈尔滨医科大学 附属第四医院 放射科，哈尔滨 150001；
3. 哈尔滨工业大学 材料科学与工程学院，哈尔滨 150001

摘 要：为了开发新型的生物医用 *β* 型钛合金，设计并采用电弧熔炼方法制备 Ti−15Mo−*x*Nb (*x*=0, 5, 10 和 15，质量分数，%) 合金，研究添加元素 Nb 对 4 种合金显微组织、力学性能和铸造性能的影响。相分析和组织观察结果表明，4 种合金均由单一的 *β* 相组成，随着 Nb 含量的增加，合金的显微组织细化。*β* 型 Ti−15Mo−*x*Nb 合金具有较高的塑性和相当低的压缩弹性模量(18.388~19.365 GPa)。添加 Nb 元素后，合金的压缩屈服强度增高，随着 Nb 含量的增加，合金的显微硬度降低。在冷压缩变形后，4 种合金均呈现明显的纤维带状组织。4 种合金的充型实验表明：添加 Nb 元素后，合金的充型能力降低，Ti−15Mo 合金的充型性能(92.01%)最好。

关键词：*β* 型钛合金；Ti−Mo−Nb；Nb；铸造性能；显微组织；力学性能

(Edited by Xiang-qun LI)